



Design, synthesis, and binding affinities of potential positron emission tomography (PET) ligands with optimal lipophilicity for brain imaging of the dopamine D₃ receptor. Part II

Marcello Leopoldo*, Enza Lacivita, Paola De Giorgio, Marialessandra Contino, Francesco Berardi, Roberto Perrone

Università degli Studi di Bari, Dipartimento Farmaco-Chimico, via Orabona, 4, 70125 Bari, Italy

ARTICLE INFO

Article history:

Received 9 September 2008

Revised 13 November 2008

Accepted 15 November 2008

Available online 24 November 2008

Keywords:

D₃ receptors

Positron emission tomography

Structure–affinity relationships

Arylpiperazine

Lipophilicity

ABSTRACT

In the search for compounds with potential for development as positron emission tomography radioligands for brain D₃ receptor imaging, a series of *N*-[4-(4-arylpiperazin-1-yl)butyl]arylcarboxamides with appropriate lipophilicity ($2 < \log P < 3.5$) were synthesized and tested in vitro. Some of the final compounds showed moderate-to-high dopamine D₃ receptor affinities but lacked selectivity over D₂ receptors.

© 2008 Elsevier Ltd. All rights reserved.

1. Introduction

Positron emission tomography (PET) is a powerful in vivo imaging technique that is showing its potential in various areas such as diagnosis, drug discovery, and target validation. This functional, nuclear imaging technique can trace the fate of radiolabeled molecules directly, but non-invasively, and allow precise pharmacokinetic and pharmacodynamic measurements. Molecular imaging provides unique data that can aid in selecting the best drug candidates, determining optimal dosing regimens, clearing regulatory hurdles and lowering risks of failure.¹ Development of suitable radioligands has allowed the visualization of several molecular targets into the central nervous system (CNS), including monoamine transporters (NET, SERT, DAT),² dopamine D₂,³ serotonin 5-HT_{1A},⁴ mGluR5,⁵ opioid,⁶ and cannabinoid CB1 receptors.⁷ Also the dopamine D₃ receptor subtype has been the target for PET tracer development. Molecular genetic studies of G-protein coupled receptors have defined two families of dopamine receptors, the D₁-like (D₁ and D₅ receptor subtypes) and D₂-like (D₂, D₃, and D₄ receptor subtypes) receptors based upon structural and pharmacological similarities.^{8,9} Various pharmacological studies have investigated the D₃ receptor as an interesting therapeutic target for the treatment of schizophrenia,^{10,11} Parkinson's disease,¹² drug-induced dyskinesia.¹³ Recent studies have shown that selective dopamine D₃ recep-

tor antagonists are efficacious in animal models of cocaine-, nicotine-, alcohol-, and heroin-seeking behaviors.¹⁴ The D₂ and D₃ dopamine receptors have approximately 46% amino acid homology. However, the transmembrane spanning regions of the D₂ and D₃ receptors, which are thought to construct the ligand binding site, share 78% homology.¹⁵ Because of the high degree of homology, it has been difficult to obtain compounds that can bind selectively to either the D₂ or the D₃ dopamine receptors.^{16,17} Various dopamine D₃ receptor ligands have been labeled with a positron emitter (compounds **1–8**, Table 1), but none of them was suitable for in vivo imaging of D₃ receptors.^{18–24} An adequate PET radioligand should fulfill a number of requirements.²⁵ The candidate radioligand should be suitable for high specific activity labeling with carbon-11 (half-life = 20.38 min) or fluorine-18 (half-life = 109.8 min). The tracer needs to have high affinity for the target receptor. In particular, it is preferable that the B_{\max} clearly exceeds the K_d of the ligands (ideally $B_{\max}/K_d > 10$). Furthermore, the selectivity over other receptors needs to be good (about 100-fold). It should not be toxic. It should cross the blood–brain barrier. This implies an appropriate lipophilicity ($\log P = 1.5–4$), low molecular weight (<450 Da), and absence of P-glycoprotein-mediated-efflux of the tracer. On the other hand, the lipophilicity should not be too high in order to avoid non-specific binding. This is an essentially non-saturable component of the total tissue uptake of a radioligand, usually attributed to adhesion to protein and lipids. Therefore, it appears that there is an optimal range of lipophilicity for brain radioligands, wherein brain uptake is high

* Corresponding author. Tel.: +39 080 5442798; fax: +39 080 5442231.
E-mail address: leopoldo@farmchim.uniba.it (M. Leopoldo).

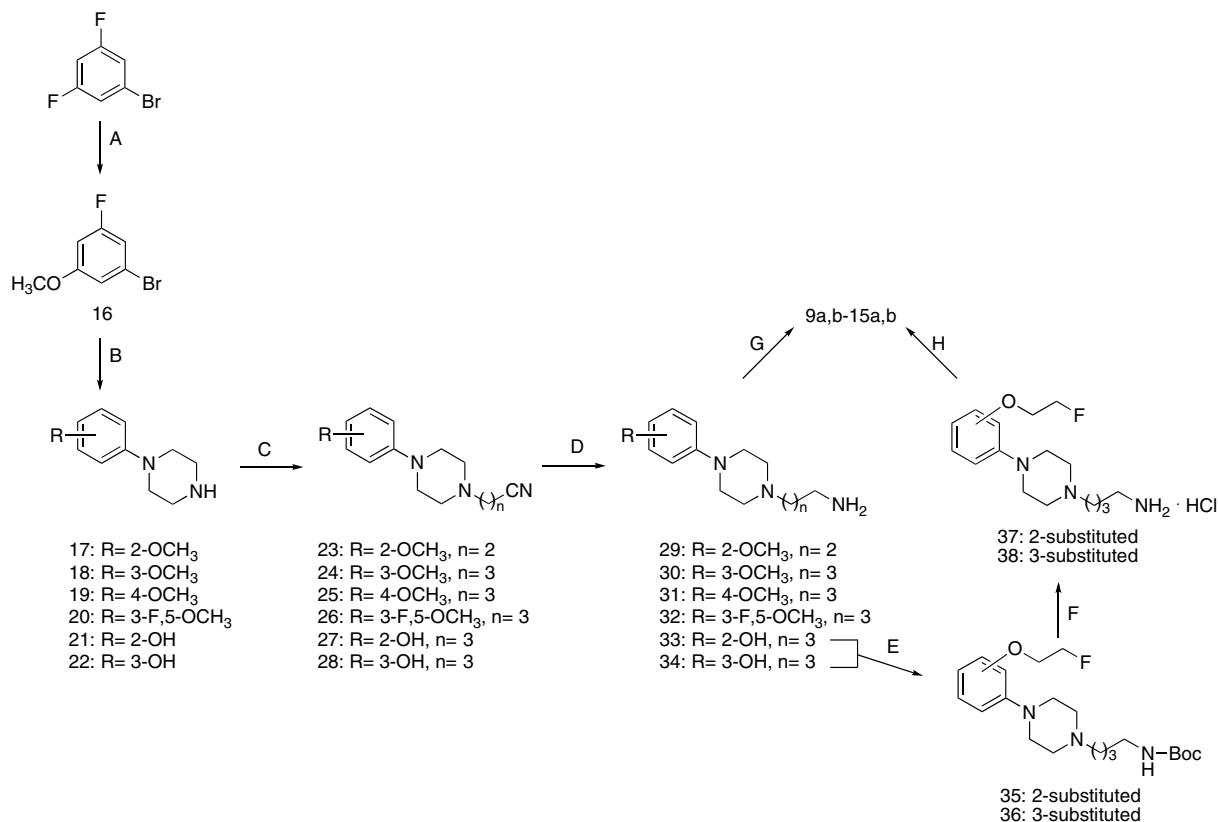
Table 1
Structures and properties of reported radiolabeled dopamine D₃ ligands

Compound	Structure	D ₃ affinity (<i>K_i</i> , nM)	Calculated log <i>P</i> values ^a	Ref.
1 (BP-897)		1.4	4.52	18
2		0.6	6.10	19
3		0.13	5.72	19
4 (FAUC346)		0.23	5.37	20
5 (2-MMC)		0.56	3.88	21
6		1.1	4.98	22
7 (RGH-1756)		0.12	3.71	23
8 (GR218231)		1.3	5.40	24

^a Calculated with ACD/Labs 7.0 (Advanced Chemistry Development, Inc., Toronto, ON, Canada).

and non-specific binding comparatively weak. From literature data a value of log *P* = 3.5 appears to be the acceptable upper limit of lipophilicity for a PET radioligand.²⁶ Finally, the radioligand metabolism should not produce radiolabeled metabolites that enter the brain. Clearly, these requirements might be conflicting, inasmuch as many chemical and pharmacologic parameters are associated with in vivo behaviors that might affect the final image qualities in opposite directions. Dopamine D₃ receptor ligands **1–8** possessed several of the above mentioned features. In fact, they displayed nanomolar to subnanomolar affinity for D₃ receptors ranging from 0.12 to 86 nM and D₂/D₃ *K_i* ratios ranging from 4.9 to >5000. However, they failed to visualize dopamine D₃ receptor in vivo due to a low signal for specific binding to the D₃ receptor (compounds **1–5**), disappointing binding characteristics in preli-

minary autoradiography experiments (compound **6**), D₃ affinity at in vivo conditions not sufficient to visualize the D₃ receptors in the brain (compound **7**), or interaction with another molecular target (compound **8**). Thus, the discovery of highly selective radioligands as PET tracers is still an important task to highlight the pathophysiological role of the D₃ receptor. In a previous paper we have described a series of potential PET radioligand for the visualization of brain dopamine D₃ receptors.²⁷ That series originated from the high affinity D₃ receptor ligand **3** through structural modifications targeted to lower lipophilicity and to leave unchanged the high affinity for D₃ receptor. A significant reduction in lipophilicity was achieved essentially by substituting the 2,3-dichlorophenyl group. However, this moiety revealed to be essential for high affinity and selectivity for D₃ receptor. Nonetheless, we



Scheme 1. Synthesis of the target compounds **9a,b–15a,b**. Reagents and conditions: (A) Sodium methoxide, DMF; (B) piperazine, sodium *t*-butoxide, dichlorobis(tri-*o*-tolylphosphine)palladium, anhydrous toluene; (C) ω -bromoalkyl nitrile, K₂CO₃ (except for **27** and **28**), acetonitrile; (D) borane–methyl sulfide complex, anhydrous THF; (E) i: di-*t*-butylcarbonate, Et₃N, H₂O, THF; ii: 2-fluoroethyl mesylate, Cs₂CO₃, DMF, 65 °C (F) 4 M HCl in dioxane, rt, 3 h. (G) carboxylic acid, 1,1'-carbonyldiimidazole, anhydrous THF, or Et₃N, methyl chloroformate; (H) carboxylic acid, PyBOP, *N*-methylmorpholine, anhydrous CH₂Cl₂.

which is the less basic compound of the series. Taken together, these data suggest that, for this class of compounds, *clogP* values are reliable for predicting the actual lipophilicity of the target molecules. Moreover, the *pK_a* values indicate that the piperazine nitrogen is not extensively protonated at physiological pH, and this should be adequately considered in the design of potential PET tracers with arylpiperazine structure.

3.2. Structure–affinity relationships

The first set of modifications performed on the reference compounds were shortening of the methylene spacer between the aryl-carboxamide moiety and the 1-(2-methoxyphenyl)piperazine (compounds **10a,b**) and shifting of the methoxy substituent from the 2-position to 3- and 4-position of the phenyl attached to the piperazine ring (compounds **11a,b–12a,b**). These structural modifications left unchanged the possibility to access to a labeled compound and also reflected into a slight reduction in lipophilicity. Shortening of the spacer (**9a** vs **10a** and **9b** vs **10b**) resulted in a reduction of D₃ affinity of different amplitude: in fact, **10a** was 15-fold less potent than **9a**, whereas **10b** was devoid of D₃ affinity. This modification had a limited impact on D₂ receptor affinity, being **10b** only twofold less potent than **9b**. Evaluation of the optimal position of the methoxy substituent was carried out because literature data suggested for similar structure type that a substituent in 3-position of the phenyl ring could leave unchanged the affinity for D₃ receptor, while reducing the affinity for dopamine D₂ receptor.²⁹ This was not replicated in the present examples: 2-methoxy substituted derivatives were more potent than the corresponding 3-methoxy isomers which were more potent than the 4-substituted ones. The difference in D₃ receptor affinity among

the isomers **9a**, **11a**, and **12a** were less marked than that observed among the isomers **9b**, **11b**, and **12b**. The same affinity trend was observed for dopamine D₂ receptor: *K_i* values at D₂ receptor of **11a,b** were approximately 10-fold higher than that of **9a,b**, respectively. Shifting of the methoxy group from 3- to 4-position gave derivatives **12a,b** which were devoid of affinity for D₂ receptors (*K_i* > 1000 nM).

The second set of structural modifications were aimed to include a fluorine atom into the structure, because fluorine-18 possess a longer half-life than carbon-11. For this purpose, we replaced the methoxy group of compounds **9a,b** and **11a,b** with a 2-fluoroethoxy substituent, leading to compounds **13a,b–14a,b**. This modification affected dopamine D₃ affinity in a narrow range, being **13a** equipotent to **9a**, and **14a** fivefold less potent than **9b**. On the other hand, **13a,b–14a** showed higher D₂ affinity as compared to their methoxy counterparts. Also, we evaluated fluoroaromatic derivatives **15a,b** which can be considered formally derived from **11a,b** by introduction of a fluorine on the phenyl ring attached to the piperazine. The 3,5-disubstitution pattern was chosen because it was already reported for other dopamine D₃ ligands.^{30,31} This modification left unchanged D₃ affinity for 4-(1*H*-imidazol-1-yl)benzamides (**11a** vs **15a**), whereas was detrimental for 2,1,3-benzoxadiazole-5-carboxamides (**11b** vs **15b**). The same trend was shown by D₂ affinity data of **15a,b** in comparison with **11a,b**.

4. Conclusions

Herein we report an attempt to identify potential PET ligands for dopamine D₃ receptors. The *N*-[4-(4-aryl)piperazin-1-yl]butyl]arylcarboxamide scaffold was modified with the aim

to combine high affinity for D₃ receptors, selectivity over D₂ receptors, appropriate lipophilicity for high brain uptake and low non-specific binding, and suitable chemical feature for carbon-11 or fluorine-18 labeling. The target compounds **9a,b**–**15a,b** presented logD_{7.4} values between 2.22 and 3.12 and, thus, within the optimal lipophilicity range. As far as the affinity for D₃ receptor is concerned, only compounds **13a**, **13b**, **14a**, and **15a** showed good binding properties, being **13a** the most potent of the series. However, the K_i value of 2.95 nM is quite below the target for optimal B_{max}/K_d ratio for D₃ receptors. Unfortunately, all the compounds showed modest selectivities over D₂ receptors. As pointed out above, the high degree of amino acid homology between the D₂ and D₃ dopamine receptor subtypes, constitutes a formidable challenge in the pursuit to discover dopamine D₃-selective compounds. Within the *N*-[4-(4-arylpiperazin-1-yl)alkyl]arylcarboxamide class, high dopamine D₂/D₃ selectivity has been achieved with lipophilic arylcarboxylamides connected through a butyl chain to a 2,3-dichloro- or 2-methoxy-substituted phenylpiperazine as in the case of compounds **1–6** (Table 1). Very recent literature data seem to confirm the above trend. During the preparation of the present manuscript, Hocke and coworkers³² have reported on four potential D₃ PET tracer structurally related to compound **13a**, where the 4-(1*H*-imidazol-1-yl)benzamide moiety was replaced by more lipophilic bicyclic systems (i.e., benzothiophene, benzofurane, pyrazolo[1,5-*a*]pyridine, naphthalene). Those compounds were reported to bind at D₃ receptors with subnanomolar affinities (K_i = 0.12–0.68 nM) and to possess about 100-fold selectivity over D₂ receptor. From these data it became apparent that maintaining potency and specificity for D₃ receptors while optimizing the physicochemical properties, is still a complex challenge.

5. Experimental

5.1. Chemistry

Column chromatography was performed with 1:30 Merck silica gel 60A (63–200 μm) as the stationary phase. Melting points were determined in open capillaries on a Gallenkamp electrothermal apparatus. Elemental analyses (C,H,N) were performed on Eurovector Euro EA 3000 analyzer; the analytical results were within ±0.4% of the theoretical values for the formula given. ¹H NMR spectra were recorded at 300 MHz on a Varian Mercury-VX spectrometer. All spectra were recorded on free bases. All chemical shift values are reported in ppm (δ). Recording of mass spectra was done on an HP6890-5973 MSD gas chromatograph/mass spectrometer; only significant *m/z* peaks, with their percentage of relative intensity in parentheses, are reported. ESI⁺/MS/MS analysis was performed with an Agilent 1100 Series LC-MSD trap System VL workstation. All spectra were in accordance with the assigned structures. The purity of new compounds that were essential to the conclusions drawn in the text was determined by HPLC on a Perkin-Elmer series 200 LC instrument using a Phenomenex Gemini RP-18 column, (250 × 4.6 mm, 5 μm particle size) and equipped with a Perkin-Elmer 785A UV/VIS detector setting λ = 254 nm. Compounds **9a,b**–**15a,b** were eluted with CH₃OH/H₂O/Et₃N, 4:1:0.01, v/v at a flow rate of 0.8 mL/min. When necessary, a standard procedure was used to transform final compounds into their hydrochloride salts. The following compounds were synthesized according to published procedures: 3-[4-(2-methoxyphenyl)piperazin-1-yl]propanenitrile (**23**),³³ 4-[4-(3-methoxyphenyl)piperazin-1-yl]butanenitrile (**24**),³⁴ 3-(2-methoxyphenyl)-1-piperazinepropanamine (**29**),³³ 4-(3-methoxyphenyl)-1-piperazinebutanamine (**30**).³⁴

5.1.1. 1-Bromo-3-fluoro-5-methoxybenzene (**16**)

To an ice-cooled solution of 1-bromo-3,5-difluorobenzene (3.00 g, 15.6 mmol) in anhydrous DMF (7 mL) was added portion-wise sodium methoxide (1.69 g, 31.2 mmol). Then, the cooling bath was removed and the reaction mixture was stirred 24 h at room temperature. Then, mixture was diluted with CH₂Cl₂ (40 mL) and washed with H₂O (40 mL). The separated organic layer was dried (Na₂SO₄) and concentrated under reduced pressure. The crude residue was chromatographed (petroleum ether as eluent) to give the title compound as a colorless oil (1.48 g, 46% yield). GC–MS *m/z* 206 (M⁺+2, 97), 204 (M⁺, 100), 176 (30), 174 (30), 95 (39). ¹H NMR (CHCl₃): δ 3.79 (s, 3H), 6.56 (dt, 1H, *J* = 2.3, 10.5 Hz), 6.82–6.87 (m, 2H).

5.1.2. 1-(3-Fluoro-5-methoxyphenyl)piperazine (**20**)

A mixture of **16** (1.48 g, 7.3 mmol), piperazine (2.49 g, 29.0 mmol), sodium *t*-butoxide (0.97 g, 10.0 mmol), dichlorobis(tri-*o*-tolylphosphine)palladium (II) (0.16 g, 0.2 mmol) in anhydrous toluene (30 mL) was warmed at 100 °C overnight. Then, the mixture was cooled, filtered through Celite, and evaporated to dryness in vacuo. The residue was taken-up with AcOEt (40 mL) and washed with H₂O (40 mL). The separated organic layer was dried (Na₂SO₄) and concentrated under reduced pressure. The crude residue was chromatographed (CHCl₃/MeOH, 9:1) to give 1-arylpiperazine **20** as a pale yellow oil (0.59 g, 39% yield). GC–MS *m/z* 211 (M⁺+1, 5), 210 (M⁺, 34), 168 (100). ¹H NMR (CHCl₃): δ 1.79 (s, 1H, D₂O exchanged), 3.00 (app q, 4H), 3.12 (app q, 4H), 3.75 (s, 3H), 6.12 (dt, 1H, *J* = 2.3, 10.5 Hz), 6.19–6.25 (m, 2H).

5.2. General procedure for preparation of nitriles **23–29**

A stirred suspension of 1-arylpiperazine **17–22** (10 mmol), ω-bromoalkylnitrile (11 mmol) and K₂CO₃ (11 mmol) (this reagent was omitted in the case of arylpiperazines **21** and **22**) in acetonitrile (50 mL) was refluxed overnight. After cooling, the mixture was evaporated to dryness and H₂O (20 mL) was added to the residue. The aqueous phase was extracted with CH₂Cl₂ (2 × 30 mL). The collected organic layers were dried over Na₂SO₄ and evaporated under reduced pressure. The crude residue was chromatographed as detailed below to yield pure **23–29** as white solids.

5.2.1. 4-[4-(4-Methoxyphenyl)piperazin-1-yl]butanenitrile (**25**)

Eluted with CHCl₃/AcOEt, 1:1. 83% Yield. GC–MS *m/z* 260 (M⁺+1, 18), 259 (M⁺, 100), 219 (36). ¹H NMR (CHCl₃): δ 1.87 (quintet, 2H, *J* = 6.9 Hz), 2.46 (t, 2H, *J* = 7.2 Hz), 2.53 (t, 2H, *J* = 6.9 Hz), 2.62 (app t, 4H), 3.10 (app t, 4H), 3.77 (s, 3H), 6.82–6.92 (m, 4H).

5.2.2. 4-[4-(3-Fluoro-5-methoxyphenyl)piperazin-1-yl]butanenitrile (**26**)

Eluted with CHCl₃/AcOEt, 1:1. 95% Yield. GC–MS *m/z* 278 (M⁺+1, 18), 277 (M⁺, 100), 237 (55), 223 (49), 123 (50). ¹H NMR (CHCl₃): δ 1.85 (quintet, 2H, *J* = 6.9 Hz), 2.45 (t, 2H, *J* = 7.2 Hz), 2.50 (t, 2H, *J* = 6.7 Hz), 2.56 (app t, 4H), 3.17 (app t, 4H), 3.76 (s, 3H), 6.12 (dt, 1H, *J* = 2.1, 5.2 Hz), 6.18–6.20 (m, 1H), 6.24 (t, 1H, *J* = 2.1 Hz).

5.2.3. 4-[4-(2-Hydroxyphenyl)piperazin-1-yl]butanenitrile (**27**)

Eluted with CHCl₃/MeOH, 19:1. 76% Yield. GC–MS *m/z* 246 (M⁺+1, 5), 245 (M⁺, 32), 205 (29), 148 (100). ¹H NMR (CHCl₃): δ 1.86 (quintet, 2H, *J* = 6.9 Hz), 2.47 (t, 2H, *J* = 7.0 Hz), 2.54 (t, 2H, *J* = 6.7 Hz), 2.58 (app t, 4H), 2.90 (app t, 4H), 6.83–6.89 (m, 1H), 6.94 (dd, 1H, *J* = 1.7, 8.8 Hz), 7.02 (br s, 1H, D₂O exchanged), 7.05–7.15 (m, 1H), 7.17 (dd, 1H, *J* = 1.7, 8.5 Hz).

5.2.4. 4-[4-(3-Hydroxyphenyl)piperazin-1-yl]butanenitrile (**28**)

Eluted with CHCl₃/MeOH, 19:1. 44% Yield. GC–MS *m/z* 246 (M⁺+1, 17), 245 (M⁺, 100), 205 (52), 191 (38). ¹H NMR (CHCl₃): δ

1.86 (quintet, 2H, $J = 6.9$ Hz), 2.45 (t, 2H, $J = 7.2$ Hz), 2.51 (t, 2H, $J = 6.7$ Hz), 2.58 (app t, 4H), 3.17 (app t, 4H), 5.36 (br s, 1H, D₂O exchanged), 6.29–6.33 (m, 1H), 6.37 (t, 1H, $J = 2.3$ Hz), 6.49 (dd, 1H, $J = 1.9, 8.2$ Hz), 7.10 (t, 1H, $J = 8.1$ Hz).

5.3. General procedure for preparation of amines 31–34

Borane–methyl sulfide complex, as 10.0 M BH₃ in excess methyl sulfide (1.2 mL, 12.0 mmol) was dropped into an ice-cooled solution of nitrile **25–28** (4.0 mmol) in anhydrous THF (10 mL), under stirring. After being refluxed for 1 h, the reaction mixture was cooled at -10 °C and MeOH was added very carefully dropwise until gas evolution ceased. The mixture was treated with 3 N HCl (5 mL) and was refluxed for 1 h. After cooling, the mixture was alkalinized with 3 N NaOH and extracted with CH₂Cl₂ (2 × 50 mL). The collected organic layers were dried over Na₂SO₄ and the solvent was evaporated under reduced pressure to give the amines **31–34** as a white semisolids which were used for the next step without further purification.

5.3.1. 4-(4-Methoxyphenyl)-1-piperazinebutanamine (31)

Quantitative yield. GC–MS m/z 264 ($M^+ + 1$, 13), 263 (M^+ , 65), 248 (32), 205 (59), 163 (93), 127 (100). ¹H NMR (CHCl₃): δ 1.44–1.64 (m, 4H), 2.25 (br s, 2H, D₂O exchanged), 2.40 (t, 2H, $J = 7.2$ Hz), 2.62 (app t, 4H), 2.74 (t, 2H, $J = 6.6$ Hz), 3.10 (app t, 4H), 3.75 (s, 3H), 6.81–6.97 (m, 4H).

5.3.2. 4-(3-Fluoro-5-methoxyphenyl)-1-piperazinebutanamine (32)

84% Yield. GC–MS m/z 281 (M^+ , 2), 208 (21), 168 (69), 91 (100). ¹H NMR (CHCl₃): δ 1.42–1.60 (m, 4H), 2.00 (br s, 2H, D₂O exchanged), 2.38 (t, 2H, $J = 6.9$ Hz), 2.56 (app t, 4H), 2.75 (t, 2H, $J = 6.2$ Hz), 3.17 (app t, 4H), 3.75 (s, 3H), 6.10 (d, 1H, $J = 10.5$ Hz), 6.19 (s, 1H), 6.21 (d, 1H, $J = 12.7$ Hz).

5.3.3. 2-[4-(4-Aminobutyl)-1-piperazinyl]phenol (33)

44% Yield. GC–MS m/z 250 ($M^+ + 1$, 3), 249 (M^+ , 10), 191 (52), 148 (48), 134 (69), 127 (100). ¹H NMR (CHCl₃): δ 1.48–1.63 (m, 4H), 2.43 (t, 2H, $J = 6.2$ Hz), 2.62 (br s, 7H), 2.74 (br s, 2H), 2.91 (br s, 4H), 6.85 (dt, 1H, $J = 1.3, 7.6$ Hz), 6.92 (dd, 1H, $J = 1.2, 8.1$ Hz), 7.06 (dt, 1H, $J = 1.3, 7.6$ Hz), 7.17 (dd, 1H, $J = 1.1, 6.6$ Hz).

5.3.4. 3-[4-(4-Aminobutyl)-1-piperazinyl]phenol (34)

46% Yield. ESI⁺/MS m/z 250 (MH^+). ESI⁺/MS/MS m/z 233 (100), 179 (28). ¹H NMR (CHCl₃): δ 1.48–1.62 (m, 4H), 2.39 (t, 2H, $J = 7.3$ Hz), 2.57 (app t, 4H), 2.75 (t, 2H, $J = 6.6$ Hz), 3.02 (br s, 3H, D₂O exchanged), 3.15 (app t, 4H), 6.29 (dd, 1H, $J = 1.6, 7.8$ Hz), 6.36 (t, 1H, $J = 2.2$ Hz), 6.44 (dd, 1H, $J = 1.9, 8.3$ Hz), 7.06 (t, 1H, $J = 8.1$ Hz).

5.3.5. *N*-*t*-Butoxycarbonyl-4-(2-(2-fluoroethoxy)phenyl)-1-piperazinebutanamine (35)

Amine **33** (0.71 g, 2.9 mmol) was solubilized in a mixture of H₂O (10 mL) and THF (30 mL). Et₃N (0.4 mL, 2.9 mmol) and di-*t*-butyl-carbonate (0.62 g, 2.9 mmol) were added to the solution. The mixture was stirred at room temperature overnight. Then, THF was evaporated in vacuo and the aqueous residue was extracted with AcOEt (3 × 20 mL). The organic phases were collected, dried over Na₂SO₄ and concentrated under reduced pressure. The crude residue was chromatographed (CHCl₃/MeOH, 19:1 as eluent) to give 0.85 g of *N*-BOC-**33** as white semisolid. A mixture of *N*-BOC-**33** (0.85 g, 2.4 mmol), 2-fluoroethyl mesylate (0.53 g, 4.9 mmol), and Cs₂CO₃ (0.48 g, 1.5 mmol) in DMF was warmed at 65 °C for 3 h. Then, the solvent was distilled off and the residue was taken-up with AcOEt (30 mL). The organic phase was washed first with H₂O (20 mL), with brine, then dried over Na₂SO₄. Evaporation of

the solvent in vacuo gave a crude residue which was chromatographed (CHCl₃/MeOH, 19:1) to afford pure **35** as a pale yellow oil (0.62 g, 65% yield). ESI⁺/MS m/z 396 (MH^+). ESI⁺/MS/MS m/z 296 (100), 279 (33), 225 (20). ¹H NMR (CHCl₃): δ 1.43 (s, 9H), 1.54–1.56 (m, 4H), 2.39 (app t, 2H), 2.95 (br s, 4H), 3.04 (br s, 2H), 3.15 (app t, 4H), 4.19–4.32 (m, 2H), 4.68–4.87 (m, 2H), 5.30 (br s, 1H), 6.83–6.88 (m, 1H), 6.91–6.99 (m, 2H), 7.02–7.09 (m, 1H).

5.3.6. *N*-*t*-Butoxycarbonyl-4-(3-(2-fluoroethoxy)phenyl)-1-piperazinebutanamine (36)

As above, starting from amine **34** the title compound was obtained in 65% yield. ESI⁺/MS m/z 396 (MH^+). ESI⁺/MS/MS m/z 296 (100), 279 (34). ¹H NMR (CHCl₃): δ 1.42 (s, 9H), 1.54–1.56 (m, 4H), 2.36 (t, 2H, $J = 6.9$ Hz), 2.58 (app t, 4H), 3.12–3.16 (m, 2H), 3.21 (app t, 4H), 4.13–4.52 (m, 2H), 4.58–4.83 (m, 2H), 5.23 (br s, 1H), 6.40 (dd, 1H, $J = 2.2, 8.0$ Hz), 6.50 (t, 1H, $J = 2.3$ Hz), 6.54–6.58 (m, 1H), 7.16 (t, 1H, $J = 8.3$ Hz).

5.3.7. 4-(2-(2-Fluoroethoxy)phenyl)-1-piperazinebutanamine (37)

A mixture of **35** (0.28 g, 0.7 mmol) and 4 M HCl in dioxane (20 mL) was stirred at room temperature 3 h. Then, the solvent was removed under reduced pressure. The obtained hydrochloride salt was dried in vacuo and used for the next step without any further purification. ESI⁺/MS m/z 296 (MH^+). ESI⁺/MS/MS m/z 279 (100), 225 (60). ¹H NMR (free base, CHCl₃): δ 1.43–1.62 (m, 6H, 2H D₂O exchanged), 2.41 (t, 2H, $J = 7.4$ Hz), 2.64 (br s, 4H), 2.72 (t, 2H, $J = 6.7$ Hz), 3.13 (app t, 4H), 4.21–4.31 (m, 2H), 4.68–4.88 (m, 2H), 6.83–6.88 (m, 1H), 6.94–6.98 (m, 3H).

5.3.8. 4-(3-(2-Fluoroethoxy)phenyl)-1-piperazinebutanamine (38)

Amine **38** hydrochloride was obtained as above starting from **36**. ESI⁺/MS m/z 296 (MH^+). ESI⁺/MS/MS m/z 279 (100), 225 (29). ¹H NMR (free base, CHCl₃): δ 1.43–1.62 (m, 4H), 1.69 (s, 2H, D₂O exchanged), 2.40 (t, 2H, $J = 7.4$ Hz), 2.59 (app t, 4H), 2.73 (t, 2H, $J = 6.7$ Hz), 3.20 (app t, 4H), 4.13–4.26 (m, 2H), 4.64–4.83 (m, 2H), 6.40 (dd, 1H, $J = 2.2, 7.7$ Hz), 6.50 (t, 1H, $J = 2.3$ Hz), 6.55–6.58 (m, 1H), 7.16 (t, 1H, $J = 8.2$ Hz).

5.4. General procedure for the synthesis of carboxamides 10a,b, 11a, 12a,b, and 15a,b

A mixture of the appropriate carboxylic acid (0.48 mmol) and 1,1'-carbonyldiimidazole (0.50 mmol) in 10 mL of anhydrous THF was stirred for 8 h. A solution of amine **29–31** (0.48 mmol) in 10 mL of anhydrous THF was added and the mixture was stirred until the carboxylic acid disappeared (TLC). The reaction mixture was partitioned between AcOEt (20 mL) and H₂O (20 mL). The separated organic layer was washed with aqueous Na₂CO₃ solution (20 mL), dried (Na₂SO₄) and concentrated in vacuo. The crude residue was chromatographed with CHCl₃/CH₃OH, 19:1, to afford the pure arylcarboxamide.

5.4.1. *N*-[4-[3-(3-Methoxyphenyl)piperazin-1-yl]propyl]-4-(1H-imidazol-1-yl)benzamide (10a)

35% Yield. GC–MS m/z 420 ($M^+ + 1$, 11), 419 (M^+ , 47), 404 (30), 257 (25), 205 (100). ¹H NMR (CHCl₃): δ 1.86–1.92 (m, 2H), 2.73 (t, 2H, $J = 5.6$ Hz), 2.79 (br s, 4H), 3.12 (br s, 4H), 3.63 (q, 2H, $J = 5.4$ Hz), 3.86 (s, 3H), 6.84–6.94 (m, 3H), 7.02–7.07 (m, 1H), 7.22 (app s, 1H), 7.27–7.29 (m, 1H), 7.40–7.44 (m, 2H), 7.86 (s, 1H), 7.99 (d, 2H, $J = 8.5$ Hz), 8.67 (br t, 1H). The hydrochloride salt melted at 187–189 °C (from MeOH/Et₂O). Anal. (C₂₄H₂₉N₅O₂·3HCl·2H₂O) C, H, N.

5.4.2. *N*-[4-[3-(2-Methoxyphenyl)piperazin-1-yl]propyl]-2,1,3-benzoxadiazole-5-carboxamide (**10b**)

41% Yield. ESI⁺/MS *m/z* 396 (MH⁺). ESI⁺/MS/MS *m/z* 204 (100), 193 (87), 147 (44). ¹H NMR (CDCl₃): δ 1.87–1.95 (m, 2H), 2.76 (t, 2H, *J* = 5.6 Hz), 2.82 (br s, 4H), 3.12 (br s, 4H), 3.65 (q, 2H, *J* = 5.5 Hz), 3.85 (s, 3H), 6.85 (d, 2H, *J* = 7.4 Hz), 6.90–6.96 (m, 1H), 7.00–7.06 (m, 1H), 7.84–7.94 (m, 2H), 8.35 (s, 1H), 9.03 (br s, 1H, D₂O exchanged). The hydrochloride salt melted at 205–207 °C (from MeOH/Et₂O), Anal. (C₂₁H₂₅N₅O₃·2HCl·0.2H₂O) C, H, N.

5.4.3. *N*-[4-[4-(3-Methoxyphenyl)piperazin-1-yl]butyl]-4-(1*H*-imidazol-1-yl)benzamide (**11a**)

21% Yield. ESI⁺/MS *m/z* 434 (MH⁺). ESI⁺/MS/MS *m/z* 247 (30), 242 (69), 171 (100). ¹H NMR (CHCl₃): δ 1.67–1.75 (m, 4H), 2.49 (t, 2H, *J* = 6.7 Hz), 2.63 (app t, 4H), 3.17 (app t, 4H), 3.47–3.54 (m, 2H), 3.77 (s, 3H), 6.41 (app t, 2H), 6.50 (dd, 1H, *J* = 2.2, 8.2 Hz), 6.94 (br s, 1H), 7.13–7.18 (m, 1H), 7.22 (app s, 1H), 7.28 (t, 1H, *J* = 1.2 Hz), 7.39–7.44 (m, 2H), 7.86–7.91 (m, 3H). The free base melted at 124–126 °C (from CHCl₃/*n*-hexane), Anal. (C₂₅H₃₁N₅O₂) C, H, N.

5.4.4. *N*-[4-[4-(4-Methoxyphenyl)piperazin-1-yl]butyl]-4-(1*H*-imidazol-1-yl)benzamide (**12a**)

35% Yield. ESI⁺/MS *m/z* 434 (MH⁺). ESI⁺/MS/MS *m/z* 247 (24), 242 (63), 171 (100). ¹H NMR (CHCl₃): δ 1.68–1.73 (m, 4H), 2.51 (t, 2H, *J* = 6.7 Hz), 2.67 (app t, 4H), 3.08 (app t, 4H), 3.47–3.57 (m, 2H), 3.75 (s, 3H), 6.79–6.87 (m, 4H), 7.02 (br t, 1H), 7.22 (app s, 1H), 7.28 (t, 1H, *J* = 1.2 Hz), 7.41–7.44 (m, 2H), 7.87–7.92 (m, 3H). The free base melted at 144–146 °C (from CHCl₃/*n*-hexane), Anal. (C₂₅H₃₁N₅O₂) C, H, N.

5.4.5. *N*-[4-[4-(4-Methoxyphenyl)piperazin-1-yl]butyl]-2,1,3-benzoxadiazole-5-carboxamide (**12b**)

54% Yield. ESI⁺/MS *m/z* 410 (MH⁺). ESI⁺/MS/MS *m/z* 247 (34), 218 (73), 193 (56), 176 (30), 147 (100). ¹H NMR (CDCl₃): δ 1.69–1.77 (m, 4H), 2.50 (t, 2H, *J* = 6.3 Hz), 2.64 (app t, 4H), 3.04 (app t, 4H), 3.52 (q, 2H, *J* = 5.9 Hz), 3.76 (s, 3H), 6.81 (s, 4H), 7.30 (br t, 1H), 7.85 (q, 2H, *J* = 8.9 Hz), 8.18 (s, 1H). The free base melted at 135–137 °C (from CHCl₃/*n*-hexane), Anal. (C₂₂H₂₇N₅O₃) C, H, N.

5.4.6. *N*-[4-[4-(3-Fluoro-5-methoxyphenyl)piperazin-1-yl]butyl]-4-(1*H*-imidazol-1-yl)benzamide (**15a**)

69% Yield. ESI⁺/MS *m/z* 452 (MH⁺). ESI⁺/MS/MS *m/z* 265 (25), 242 (72), 171 (100). ¹H NMR (CHCl₃): δ 1.62–1.77 (m, 4H), 2.48 (t, 2H, *J* = 6.9 Hz), 2.60 (app t, 4H), 3.15 (app t, 4H), 3.50 (q, 2H, *J* = 6.1 Hz), 3.74 (s, 3H), 6.09–6.21 (m, 3H), 6.89 (br t, 1H), 7.21 (t, 1H, *J* = 1.1 Hz), 7.29 (t, 1H, *J* = 1.4 Hz), 7.40–7.44 (m, 2H), 7.87–7.92 (m, 3H). The free base melted at 144–146 °C (from CHCl₃/*n*-hexane), Anal. (C₂₅H₃₀FN₅O₂) C, H, N.

5.4.7. *N*-[4-[4-(3-Fluoro-5-methoxyphenyl)piperazin-1-yl]butyl]-2,1,3-benzoxadiazole-5-carboxamide (**15b**)

57% Yield. ESI⁺/MS *m/z* 428 (MH⁺). ESI⁺/MS/MS *m/z* 265 (34), 218 (86), 211 (31), 176 (21), 147 (100). ¹H NMR (CDCl₃): δ 1.67–1.77 (m, 4H), 2.52 (t, 2H, *J* = 6.9 Hz), 2.63 (app t, 4H), 3.17 (app t, 4H), 3.53 (q, 2H, *J* = 6.1 Hz), 3.76 (s, 3H), 6.10–6.19 (m, 3H), 7.15 (br t, 1H), 7.82–7.91 (m, 2H), 8.20 (t, 1H, *J* = 1.1 Hz). The free base melted at 129–131 °C (from CHCl₃/*n*-hexane), Anal. (C₂₂H₂₆FN₅O₃) C, H, N.

5.5. General procedure for the synthesis of carboxamides **13a,b** and **14a,b**

A mixture of **37** or **38** hydrochloride (0.65 mmol), appropriate carboxylic acid (0.65 mmol), benzotriazol-1-yl-oxytriethylphosphonium hexafluorophosphate (0.97 mmol), and *N*-methyl

morpholine (2.6 mmol) in 10 mL of anhydrous CH₂Cl₂ was stirred overnight. Then, the mixture was washed with saturated aqueous NaHCO₃ (10 mL). The organic layer was separated, dried (Na₂SO₄) and concentrated in vacuo. The crude residue was chromatographed with CHCl₃/CH₃OH, 19:1, to afford the pure arylcarboxamide.

5.5.1. *N*-[4-[4-(2-(2-Fluoroethoxy)phenyl)piperazin-1-yl]butyl]-4-(1*H*-imidazol-1-yl)benzamide (**13a**)

57% Yield. ESI⁺/MS *m/z* 466 (MH⁺). ESI⁺/MS/MS *m/z* 279 (36), 242 (90), 225 (29), 171 (100). ¹H NMR (CHCl₃): δ 1.72–1.80 (m, 4H), 2.64 (t, 2H, *J* = 6.8 Hz), 2.83 (br s, 4H), 3.18 (br s, 4H), 3.46–3.55 (m, 2H), 4.18–4.30 (m, 2H), 4.67–4.86 (m, 2H), 6.84–6.89 (m, 2H), 6.91–7.02 (m, 2H), 7.22 (s, 1H), 7.25 (br s, 1H), 7.29–7.30 (m, 1H), 7.43 (d, 2H, *J* = 8.5 Hz), 7.87 (br s, 1H), 7.96 (d, 2H, *J* = 8.5 Hz). The free base melted at 92–93 °C (from CHCl₃/*n*-hexane), Anal. (C₂₆H₃₂FN₅O₂) C, H, N.

5.5.2. *N*-[4-[4-(2-(2-Fluoroethoxy)phenyl)piperazin-1-yl]butyl]-2,1,3-benzoxadiazole-5-carboxamide (**13b**)

38% Yield. ESI⁺/MS *m/z* 442 (MH⁺). ESI⁺/MS/MS *m/z* 279 (40), 225 (90), 218 (90), 182 (33), 147 (100). ¹H NMR (CHCl₃): δ 1.74–1.79 (m, 4H), 2.52 (t, 2H, *J* = 6.6 Hz), 2.68 (br s, 4H), 3.07 (br s, 4H), 3.52 (q, 2H, *J* = 5.6 Hz), 4.17–4.29 (m, 2H), 4.66–4.85 (m, 2H), 6.75 (m, 2H), 6.89–7.00 (m, 2H), 7.47 (br t, 1H), 7.83–7.91 (m, 2H), 8.21 (t, 1H, *J* = 1.1 Hz). The free base melted at 104–107 °C (from CHCl₃/*n*-hexane), Anal. (C₂₃H₂₈FN₅O₃) C, H, N.

5.5.3. *N*-[4-[4-(3-(2-Fluoroethoxy)phenyl)piperazin-1-yl]butyl]-4-(1*H*-imidazol-1-yl)benzamide (**14a**)

48% Yield. ESI⁺/MS *m/z* 466 (MH⁺). ESI⁺/MS/MS *m/z* 279 (30), 242 (71), 171 (100). ¹H NMR (CHCl₃): δ 1.68–1.75 (m, 4H), 2.51 (t, 2H, *J* = 6.7 Hz), 2.65 (app t, 4H), 3.18 (app t, 4H), 3.51 (q, 2H, *J* = 6.1 Hz), 4.12–4.24 (m, 2H), 4.64–4.82 (m, 2H), 6.41 (dd, 1H, *J* = 2.3, 8.1 Hz), 6.46 (t, 1H, *J* = 2.3 Hz), 6.53 (dd, 1H, *J* = 2.3, 8.2 Hz), 6.97 (br t, 1H), 7.16 (t, 1H, *J* = 8.1 Hz), 7.21 (t, 1H, *J* = 1.1 Hz), 7.26–7.29 (m, 1H), 7.40–7.45 (m, 2H), 7.86–7.91 (m, 3H). The free base melted at 118–120 °C (from CHCl₃/*n*-hexane), Anal. (C₂₆H₃₂FN₅O₂) C, H, N.

5.5.4. *N*-[4-[4-(3-(2-Fluoroethoxy)phenyl)piperazin-1-yl]butyl]-2,1,3-benzoxadiazole-5-carboxamide (**14b**)

70% Yield. ESI⁺/MS *m/z* 442 (MH⁺). ESI⁺/MS/MS *m/z* 279 (41), 225 (53), 218 (82), 176 (20), 147 (100). ¹H NMR (CDCl₃): δ 1.67–1.76 (m, 4H), 2.48 (t, 2H, *J* = 6.7 Hz), 2.61 (app t, 4H), 3.13 (br s, 4H), 3.51 (q, 2H, *J* = 6.1 Hz), 4.13–4.25 (m, 2H), 4.65–4.84 (m, 2H), 6.38–6.44 (m, 2H), 6.47–6.51 (m, 1H), 7.14 (t, 1H, *J* = 8.1 Hz), 7.43 (br t, 1H, D₂O exchanged), 7.86 (t, 2H, *J* = 1.1 Hz), 8.23 (t, 1H, *J* = 1.2 Hz). The free base melted at 83–87 °C (from CHCl₃/*n*-hexane), Anal. (C₂₃H₂₈FN₅O₃) C, H, N.

5.5.5. *N*-[4-[4-(3-Methoxyphenyl)piperazin-1-yl]butyl]-2,1,3-benzoxadiazole-5-carboxamide (**11b**)

A mixture of carboxylic acid (0.25 g, 1.5 mmol) in CHCl₃ (10 mL) and triethylamine (0.24 mL, 1.7 mmol) was stirred at room temperature for 15 min. After cooling at –10 °C methyl chloroformate (0.13 mL, 1.7 mmol) was added and the mixture reacted at the same temperature for 1 h. Then a solution of 4-(3-methoxyphenyl)-1-piperazinebutanamine (**30**) (0.44 g, 1.7 mmol) in CHCl₃ was dropped into and the resulting mixture was kept at –10 °C to –5 °C for 1 h. After stirring overnight at room temperature, the reaction mixture was washed with 5% aqueous NaOH, with water and dried over Na₂SO₄. Evaporation of the solvent in vacuo afforded the crude product which was purified by column chromatography (eluent CHCl₃/MeOH, 19:1) to give **11b** as a yellow solid (0.23 g, 37% yield). GC–MS *m/z* 410 (M⁺+1, 16), 409 (M⁺, 55), 394

(24), 205 (100). ^1H NMR (CDCl_3): δ 1.68–1.77 (m, 4H), 2.50 (t, 2H, $J = 6.7$ Hz), 2.64 (app t, 4H), 3.15 (app t, 4H), 3.52 (q, 2H, $J = 6.1$ Hz), 3.78 (s, 3H), 6.38–6.48 (m, 3H), 7.15 (t, 1H, $J = 8.1$ Hz), 7.23 (br t, 1H), 7.81–7.90 (m, 2H), 8.19 (t, 1H, $J = 1.1$ Hz). The free base melted at 119–121 °C (from CHCl_3/n -hexane), Anal. ($\text{C}_{22}\text{H}_{27}\text{N}_5\text{O}_3$) C, H, N.

5.6. Lipophilicity data

Lipophilicity data of compounds **9a,b**–**15a,b** were obtained by the pH metric technique using a GlpK_a apparatus (Sirius Analytical Instruments Ltd, Forrest Row, East Sussex, United Kingdom) as described elsewhere.^{35–38} The low aqueous solubility of the investigated compounds required pK_a measurements to be performed in the presence of methanol as co-solvent. Three separate 20 mL-semiaqueous solutions of approximately 5×10^{-5} M, in 20–40% w/w of MeOH, were initially acidified with 0.5 M HCl to pH 3.0. The solutions were then titrated with 0.5 M KOH to pH 11. The initial estimates of the p_sK_a values, which are the apparent ionization constants in the mixed solvent, were obtained by Bjerrum plots. These values were then refined by a weighted nonlinear least-squares procedure (Refinement Pro 1.0 software) to create a multi-set, where the refined values were extrapolated to zero co-solvent concentration using the Yasuda–Shedlovsky equation.³⁹ To obtain logP data, at least three separate titrations were performed on each compound, on approximately 5×10^{-5} M, in the presence of different volumes of *n*-octanol (ratios ranging from 0.005 to 1). The biphasic solutions were initially acidified to pH 3.0 with 0.5 M HCl and then titrated with 0.5 M KOH to pH 11. The obtained data were refined as described above. The logP values were obtained by the Multiset approach, as described elsewhere.^{36,37} All titrations were carried out at 25 ± 0.1 °C under an inert nitrogen gas atmosphere to exclude CO₂.

5.7. Biological methods

5.7.1. General

For receptor binding studies, the compounds were dissolved in absolute ethanol. Quinpirole was purchased from Sigma–Aldrich (Milan, Italy); [^3H]spiroperidol was obtained from PerkinElmer (Milan, Italy); haloperidol was purchased from Tocris Bioscience (Bristol, UK).

5.7.2. Radioligand binding assay at human cloned D₂ dopaminergic receptors

Binding of [^3H]spiroperidol at human cloned receptors was performed according to Scarselli et al. with some modifications.⁴⁰ The incubation buffer (5.0 mM MgCl₂, 50 mM Tris, pH 7.4) contained 4 μg of dopamine dilute membranes, 1.0 nM [^3H]spiroperidol ($K_d = 0.54$ nM) and six to nine concentrations of drug solution in a final volume of 500 μL. The samples were incubated for 30 min at 25 °C, then the incubation was stopped by rapid filtration through Whatman GF/C glass fiber filters (presoaked in 0.5% polyethylenimine for 120 min). The filters were washed with 2×4.0 mL of ice-cold incubation buffer. Non-specific binding was determined in the presence 10 μM quinpirole. The radioactivity bound to the filters was measured by liquid scintillation using LS6500 Multi-Purpose scintillation Counter, Beckman.

5.7.3. Radioligand binding assay at human cloned D_{2L} dopaminergic receptors

Binding of [^3H]spiroperidol at human cloned receptors was performed according to Scarselli et al.⁴⁰ with minor modifications. The incubation buffer (120 mM NaCl, 5.0 mM KCl, 5.0 mM MgCl₂, 1 mM EDTA, 50 mM Tris, pH 7.4) contained 100 μg of dopamine dilute membranes, 0.30–0.50 nM [^3H]spiroperidol ($K_d = 0.093$ nM) and

six to nine concentrations of drug solution in a final volume of 500 μL. The samples were incubated for 120 min at 25 °C, then the incubation was stopped by rapid filtration through Whatman GF/C glass fiber filters (presoaked in 0.5% polyethylenimine for 60 min). The filters were washed 3×1 mL of ice-cold 50 mM Tris, 0.9% NaCl, pH 7.4. Non-specific binding was determined in the presence of 10 μM haloperidol. The radioactivity bound to the filters was measured by liquid scintillation using LS6500 Multi-Purpose scintillation Counter, Beckman.

5.7.4. Statistical analysis

The inhibition curves on the different binding sites of the compounds reported in Table 2 were analyzed by nonlinear curve fitting utilizing the GraphPad Prism program.⁴¹ The value for the inhibition constant, K_i , was calculated by using the Cheng–Prusoff equation.⁴²

Supplementary data

Supplementary data associated with this article can be found, in the online version, at [doi:10.1016/j.bmc.2008.11.044](https://doi.org/10.1016/j.bmc.2008.11.044).

References and notes

- Lee, C. M.; Farde, L. *Trends Pharmacol. Sci.* **2006**, *27*, 310.
- Guilloteau, D.; Chalon, S. *Curr. Pharm. Des.* **2005**, *11*, 3237.
- de Paulis, T. *Curr. Pharm. Des.* **2003**, *9*, 673.
- Kumar, J. S.; Mann, J. J. *Drug Discovery Today* **2007**, *12*, 748.
- Yu, M. *Curr. Top. Med. Chem.* **2007**, *7*, 1800.
- Lever, J. R. *Curr. Pharm. Des.* **2007**, *13*, 33.
- Yasuno, F.; Brown, A. K.; Zoghbi, S. S.; Krushinski, J. H.; Chernet, E.; Tauscher, J.; Schaus, J. M.; Phebus, L. A.; Chesterfield, A. K.; Felder, C. C.; Gladding, R. L.; Hong, J.; Halldin, C.; Pike, V. W.; Innis, R. B. *Neuropsychopharmacology* **2008**, *33*, 259.
- Sibley, D. R.; Monsma, F. J., Jr.; Shen, Y. *Int. Rev. Neurobiol.* **1993**, *35*, 391.
- Sealfon, S. C.; Olanow, C. W. *Trends Neurosci.* **2000**, *23*, S34.
- Richtand, N. M.; Woods, S. C.; Berger, S. P.; Strakowski, S. M. *Neurosci. Biobehav. Rev.* **2001**, *25*, 427.
- Joyce, J. N.; Millan, M. J. *Drug Discovery Today* **2005**, *10*, 917.
- Joyce, J. N.; Ryoo, H. L.; Beach, T. B.; Caviness, J. N.; Stacy, M.; Gurevich, E. V.; Reiser, M.; Adler, C. H. *Brain Res.* **2002**, *955*, 138.
- Bezard, E.; Ferry, S.; Mach, U.; Stark, H.; Leriche, L.; Boraud, T.; Gross, C.; Sokoloff, P. *Nat. Med.* **2003**, *9*, 762.
- Heidbreder, C. A.; Gardner, E. L.; Xi, Z.-X.; Thanos, P. K.; Mugnaini, M.; Hagan, J. J.; Ashby, C. R. *Brain Res. Rev.* **2005**, *49*, 77.
- Sokoloff, P.; Giros, B.; Martres, M. P.; Bouthenet, M. L.; Schwarz, J. C. *Nature* **1990**, *347*, 72.
- Luedtke, R. R.; Mach, R. H. *Curr. Pharm. Des.* **2003**, *9*, 643.
- Boeckler, F.; Gmeiner, P. *Biochim. Biophys. Acta* **2007**, *1768*, 871.
- Huang, Y.; Martinez, D.; Simpson, N.; Guo, N.; Montoya, J.; Laruelle, M. *Abstracts Soc. Neurosci.* **2000**, abstr. # 809.9, p 2154.
- Turolla, E. A.; Matarrese, M.; Belloli, S.; Moresco, R. M.; Simonelli, P.; Todde, S.; Fazio, F.; Magni, F.; Galli Kienle, M.; Leopoldo, M.; Berardi, F.; Colabufio, N. A.; Lacivita, E.; Perrone, R. *J. Med. Chem.* **2005**, *48*, 7018.
- Kuhnast, B.; Valette, H.; Besret, L.; Demphel, S.; Coulon, C.; Ottaviani, M.; Guillermier, M.; Bottlaender, M.; Dollé, F. *Nucl. Med. Biol.* **2006**, *33*, 785.
- Gao, M.; Mock, B. H.; Hutchins, G. D.; Zheng, Q.-H. *Bioorg. Med. Chem.* **2005**, *13*, 6233.
- Hocke, C.; Prante, O.; Löber, S.; Hübner, H.; Gmeiner, P.; Kuwert, T. *Bioorg. Med. Chem. Lett.* **2008**, *15*, 4819.
- Sóvágó, J.; Farde, L.; Halldin, C.; Langer, O.; Laszlovszky, I.; Kiss, B.; Gulyás, B. *Neurochem. Int.* **2004**, *45*, 609.
- de Vries, E. F.; Kortekaas, R.; van Waarde, A.; Dijkstra, D.; Elsinga, P. H.; Vaalburg, W. J. *Nucl. Med.* **2005**, *46*, 1384.
- Laruelle, M.; Slifstein, M.; Huang, Y. *Mol. Imaging Biol.* **2003**, *5*, 363.
- Waterhouse, R. N. *Mol. Imaging Biol.* **2003**, *5*, 376.
- Leopoldo, M.; Lacivita, E.; De Giorgio, P.; Colabufio, N. A.; Niso, M.; Berardi, F.; Perrone, R. *J. Med. Chem.* **2006**, *49*, 358.
- Shealy, Y. F.; Krauth, C. A.; Struck, R. F.; Montgomery, J. A. *J. Med. Chem.* **1983**, *26*, 1168.
- Gyertyán, I.; Kiss, B.; Gál, K.; Laszlovszky, I.; Horváth, A.; Gémesi, L. I.; Sággy, K.; Pásztor, G.; Jájer, M.; Kapás, M.; Csongor, E. A.; Domány, G.; Tihanyi, K.; Szombathelyi, Z. *J. Pharmacol. Exp. Ther.* **2007**, *320*, 1268.
- Haupt, A.; Grandel, R.; Braje, W.; Geneste, H.; Drescher, K.; Starck, D.; Teschendorf, H.-J. *Chem. Abstr.* **2004**, *142*, 38277.
- Unger, L.; Haupt, A.; Beyerbach, A.; Drescher, K.; Braje, W.; Darbyshire, J.; Turner, S. C.; Backfisch, G. *Chem. Abstr.* **2006**, *145*, 46089.

32. Hocke, C.; Prante, O.; Salama, I.; Hübner, H.; Löber, S.; Kuwert, T.; Gmeiner, P. *Chem. Med. Chem.* **2008**, 3, 788.
33. Perrone, R.; Berardi, F.; Leopoldo, M.; Tortorella, V.; Lograno, M. D.; Daniele, E.; Govoni, S. *Farmaco* **1995**, 50, 505.
34. Campiani, G.; Butini, S.; Fattorusso, C.; Trotta, F.; Franceschini, S.; De Angelis, M.; Nielsen, K. *Chem. Abstr.* **2006**, 145, 14551.
35. Comer, J. E.; Tam, K. Y. In *Pharmacokinetic Optimization in Drug Research*; Testa, B., van de Waterbeemd, H., Folkers, G., Guy, R. H., Eds.; Wiley-VCH: Zürich, 2001; pp 275–304.
36. Avdeef, A. *Quant. Struct.-Act. Relat.* **1992**, 11, 510.
37. Avdeef, A. J. *Pharm. Sci.* **1993**, 82, 183.
38. Avdeef, A. In *Lipophilicity in Drug Action and Toxicology*; Pilska, V., Testa, B., van de Waterbeemd, H., Eds.; VCH Publishers: Weinheim, 1996; pp 109–139.
39. Avdeef, A.; Box, K. J.; Comer, J. E.; Gilges, M.; Hadley, M.; Hibbert, C.; Patterson, W.; Tam, K. Y. *J. Pharm. Biomed. Anal.* **1999**, 20, 631.
40. Scarselli, M.; Novi, F.; Schallmach, E.; Lin, R.; Baragli, A.; Colzi, A.; Griffon, N.; Corsini, G. U.; Sokoloff, P.; Levenson, R.; Vogel, Z.; Maggio, R. *J. Biol. Chem.* **2001**, 276, 30308.
41. GraphPad Prism Software (version for Windows), GraphPad Software, Inc., San Diego, CA, USA.
42. Cheng, Y. C.; Prusoff, W. H. *Biochem. Pharmacol.* **1973**, 22, 3099.